

# Synthesis of Phase Transferable Graphene Sheets Using Ionic Liquid Polymers

TaeYoung Kim,<sup>†</sup> HyunWook Lee,<sup>†</sup> JongEun Kim,<sup>‡</sup> and Kwang S. Suh<sup>†,‡,\*</sup>

<sup>†</sup>Department of Materials Science and Engineering, Korea University, 5-1 Anam-dong, Seongbuk-gu, Seoul 137-713, South Korea, and <sup>‡</sup>R&D Team, InsCon Tech, Co. Ltd, 52-12 Baekto-ri, Hyangnam-myeon, Hwaseong-si, Gyeonggi-do, 445-924, South Korea

**ABSTRACT** A practical route to the production of solution phase transferable graphene sheets using ionic liquid polymers (PIL) as a transferring medium is developed. Chemically converted graphene sheets decorated with PIL were found to be stable against the chemical reduction and well dispersed in the aqueous phase without any agglomeration. Upon the anion exchange of the PIL on graphene sheets, these PIL-modified graphene sheets in aqueous phase are readily transferred into the organic phase by changing their properties from hydrophilic to hydrophobic.

**KEYWORDS:** graphene sheets · graphene oxide · ionic liquid polymers · phase transfer

Graphene represents a new class of two-dimensional carbon nanostructure, which is a single layer of carbon atoms in a hexagonal lattice, that could potentially be utilized in electronic devices such as field-effect transistors, ultrasensitive sensors, and electromechanical resonators.<sup>1–4</sup> Although remarkable properties such as high values of mechanical strength (fracture strength, 125 GPa),<sup>5</sup> thermal conductivity ( $\sim 5000 \text{ W m}^{-1} \text{ K}^{-1}$ ),<sup>6</sup> mobility of charge carriers ( $200\,000 \text{ cm}^2 \text{ V}^{-1} \text{ s}^{-1}$ ),<sup>7</sup> and specific surface area (calculated value,  $2630 \text{ m}^2 \text{ g}^{-1}$ )<sup>8</sup> have been reported for graphene sheets, the technological development of graphene sheets is hampered because of the lack of an efficient approach for producing processable graphene sheets in large quantities.<sup>9</sup> Graphene sheets have been prepared using various methods including mechanical cleavage of graphite,<sup>2</sup> epitaxial growth using chemical vapor deposition,<sup>10</sup> and thermal fusion of polycyclic aromatic hydrocarbons.<sup>11</sup> However, the low productivity of these methods makes them unsuitable for large-scale use.<sup>12</sup> Thus, the most promising route for the bulk production of these sheets is the exfoliation of graphite in the liquid phase to form single- or few-layered graphene sheets. The most

common technique has been the oxidation and subsequent exfoliation of graphite to make graphene oxide.<sup>12</sup> This solution-based route involves the chemical oxidation of graphite to hydrophilic graphite oxide, which can be readily exfoliated as individual graphene oxide (GO) sheets in water utilizing the electrostatic repulsion of the negatively charged oxygen groups on the graphene surface. Graphene oxide, which is electrically insulating, can be restored to conducting graphene by removing the oxygen containing groups on the basal plane and edges using reducing agents such as hydroquinone,  $\text{NaBH}_4$ , and hydrazine. However, the graphene sheets obtained through the chemical conversion method tend to form irreversible agglomerates through van der Waals interaction, making further processing difficult.<sup>13</sup> Thereby, the prevention of aggregation is of particular importance for most of proposed applications of graphene sheets to be realized.

Considerable efforts have been devoted to dispersing graphene sheets in water using pH-controlled reduction of the GO dispersion<sup>14</sup> or stabilizing reduced GO sheets with polymeric or surfactant dispersants such as poly(sodium 4-styrenesulfonate),<sup>15</sup> pyrene butyrate,<sup>16</sup> and ssDNA.<sup>17</sup> Further attempts to produce isolated graphene sheets in organic solvents have also been made using particular solvents such as *N,N*-dimethylformamide, *N*-methyl-pyrrolidone, and tetrahydrofuran.<sup>18,19</sup> More recently, ionic liquids (ILs) have been proposed as an effective medium for the exfoliation of graphene sheets directly from graphite anode.<sup>20,21</sup> Even though all of these routes have successfully provided graphene nanosheets in water or certain organic solvents, the production of a stable dispersion

\*Address correspondence to suhkwang@korea.ac.kr.

Received for review October 30, 2009 and accepted February 10, 2010.

Published online February 16, 2010.  
10.1021/nn901525e

© 2010 American Chemical Society

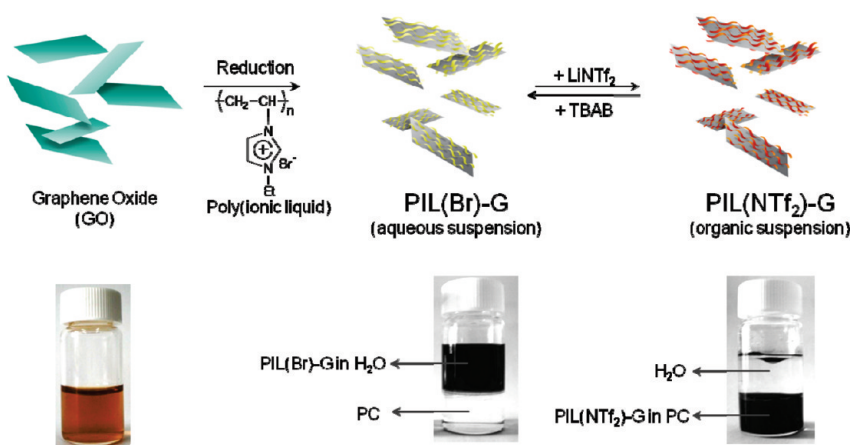
of graphene in a wide range of dispersing medium still remains challenging for the fabrication of graphene-based devices. The successful dispersion of graphene sheets would enable the use of low-cost solution processing techniques such as drop-casting, spraying, and dip- or spin-coating to fabricate graphene-based materials and further broaden their application in organic electronics utilizing graphene sheets as the active layers.

Herein, we introduce a procedure that allows the reversible phase transfer of graphene sheets between water and organic solvents. In this procedure, we used ionic liquid polymers (or polymerized ionic liquid, PIL) to stabilize the isolated graphene sheets and provide a functionality for transferring graphene sheets between the aqueous and organic phases. This work was an extension of previous demonstrations for imidazolium-based PIL that showed a tunable solubilizing characteristic with respect to the types of anions coupled with imidazolium polycations and thus can be utilized as the phase transferring vehicles for nanomaterials, which has been recognized in  $\pi$ -conjugated polymers<sup>22,23</sup> and single-walled carbon nanotubes.<sup>24</sup> Specifically, poly(1-vinyl-3-ethylimidazolium) salts were synthesized and exploited as functional materials that were capable of forming a complex with graphene sheets and switching surface properties of the graphene sheets from a hydrophilic to a hydrophobic phase. The graphene sheets were reversibly transferred between aqueous and organic solutions through a simple anion exchange treatment of PILs.

## RESULTS AND DISCUSSION

The production of phase transferable graphene sheets was achieved through the sequential chemical reactions in Scheme 1 (see Methods section). In the first step, an aqueous suspension of GO was prepared by the exfoliation of graphite through chemical oxidation. The yellowish color of GO suspension is characteristic of highly oxidized and fully suspended GO sheets.

In the second step, GO sheets suspended in water were modified with a hydrophilic ionic liquid polymer which consists of an imidazolium polycation and a bromide anion, that is, PIL(Br). A black and homogeneous suspension of PIL(Br)-modified graphene sheets, PIL(Br)-G, was then obtained in water by chemical reduction with hydrazine monohydrate. This aqueous PIL(Br)-G suspension was stable for more than 6 months, while the reduced GO without PIL(Br) precipitated out from solution within 10 min in the control experiment. This observation indicates that PIL plays an important role in stabilizing graphene sheets in aqueous



**Scheme 1.** Schematic illustration of the synthetic process for the PIL-modified graphene sheets (PIL-G). Chemical reduction of the graphene oxide (GO) dispersion with hydrazine in the presence of water-soluble PIL(Br) produced a stable aqueous suspension of the PIL(Br)-G. Anion exchange of PIL leads to the phase transfer of PIL-modified graphene sheets between aqueous and organic solvent media (propylene carbonate).

ous solution without aggregation during the reduction process. It should be also noted that the polymeric form of ionic liquid ( $M_w$  of PIL  $\approx$  170 000) is important to effectively stabilize the graphene sheets, since the use of ionic liquid monomer led to significant aggregation of graphene sheets during the chemical reduction.

In the next step, a phase transfer process was carried out to obtain PIL-modified graphene sheets in organic solvents. Interestingly, an aqueous suspension of PIL(Br)-G was readily transferred into an organic phase by exchanging the counteranion of PIL onto the graphene sheets. When an equivalent mole of lithium bis(trifluoromethylsulfonyl) amide ( $\text{Li}^+ \text{NTf}_2^-$ ) was added into the aqueous suspension of PIL(Br)-G, black precipitates were formed in water by an immediate substitution of the hydrophilic anions ( $\text{Br}^-$ ) with hydrophobic anions ( $\text{NTf}_2^-$  or  $\text{CF}_3\text{SO}_2-\text{N}-\text{SO}_2\text{CF}_3$ ) in the PIL. The resulting hydrophobic PIL( $\text{NTf}_2$ )-modified graphene sheets, PIL( $\text{NTf}_2$ )-G, were isolated and readily redispersed in a wide range of polar aprotic solvents such as propylene carbonate (PC), dimethylformamide (DMF), acetonitrile (AN), tetrahydrofuran (THF), *N*-methyl-pyrrolidone (NMP), and nitromethane (NM). These organic solvent suspensions of PIL( $\text{NTf}_2$ )-G also remain dispersed for over 6 months. Furthermore, PIL( $\text{NTf}_2$ )-G suspended in the organic solvents was reversibly transferred from the organic phase to the aqueous phase in a similar manner through the addition of appropriate salts containing hydrophilic anions such as tetrabutylammonium bromide (TBAB) or tetrabutylphosphonium bromide (TBPB). Therefore, the reversible phase transfer of graphene sheets between aqueous and organic phase has been accomplished by the simple anion exchange treatment of PILs.

The PIL-G sheets suspended in either aqueous or organic solutions were deposited onto a variety of substrates and were characterized by a number of physical methods that clearly demonstrated the production

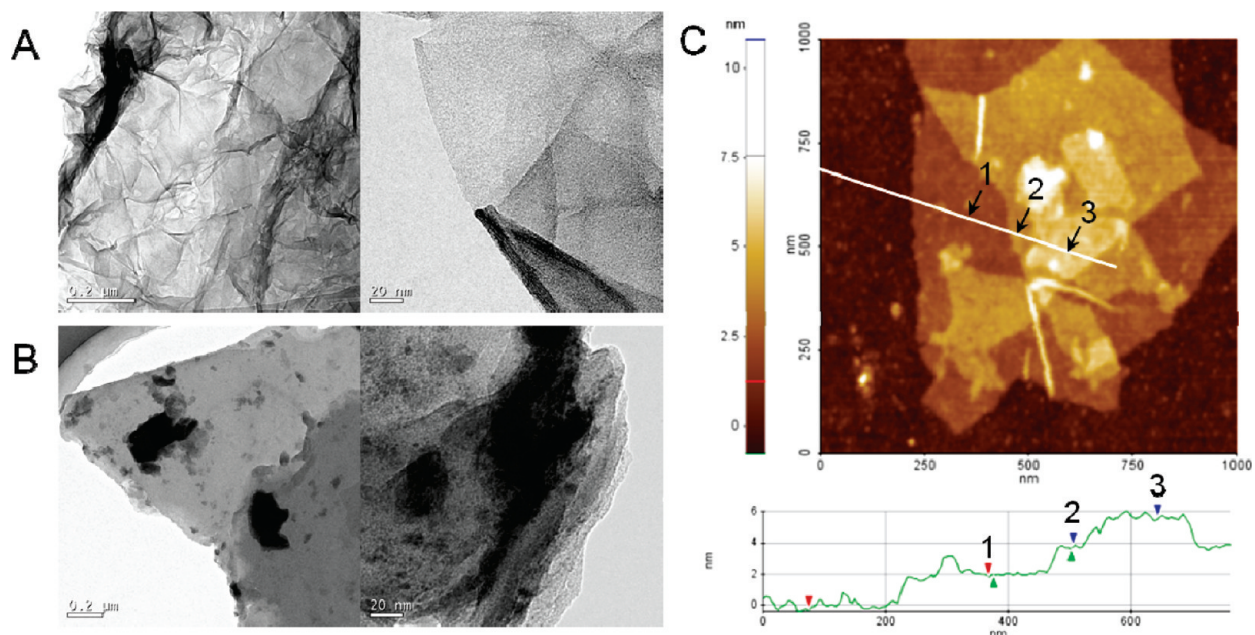


**Figure 1.** TEM images of the chemically converted graphene sheets (a) in the presence of and (b) in the absence of PIL; (c) tapping mode AFM image of the PIL-G processed from organic suspension. Height profiles across the PIL-G sheets indicating the thickness of  $\sim 1.9$  nm.

of single- or few-layered graphene sheets. The level of exfoliation of the dispersed graphene samples was characterized using transmission electron microscopy (TEM) as shown in Figure 1 a,b. The TEM image of PIL-G revealed the presence of thin graphene layers with occasional folding while large objects with a thickness of more than a few layers were rarely observed. In contrast, the reduced GO without PIL was composed of thick plates with a multilayered structure near the edges because of the agglomeration that occurred during the reduction.

The specimens for the atomic force microscopy (AFM) were prepared by drop-casting the PIL-G suspension ( $1.5 \text{ mg mL}^{-1}$ ) onto a silicon wafer substrate. Figure 1c shows a typical AFM image collected in the tapping mode displaying the morphology and thickness of the PIL-G sheet. The AFM image showed that PIL-G sheets of different lateral dimensions are stacked with each other, and the corresponding line-scan indicated that the average thickness of PIL-G was 1.9 nm. Our result showed that the thickness of PIL-G is much larger than the reported value ( $\sim 1$  nm) of GO monolayer fabricated from the water suspension.<sup>9,12</sup> This result could be attributed to the adsorbed PILs of large molecular dimension on both surfaces of the single graphene sheets.

The formation of stable PIL-G suspension allows the reaction to be monitored by UV-vis spectroscopy, and the results are shown in Figure 2a. The GO suspension displayed an absorption maximum at 230 nm, while the reduced GO and PIL(Br)-G suspension in water showed a bathochromic shift of the absorption peak to 270 nm upon reduction, along with an increase in the background absorbance. This result suggests that

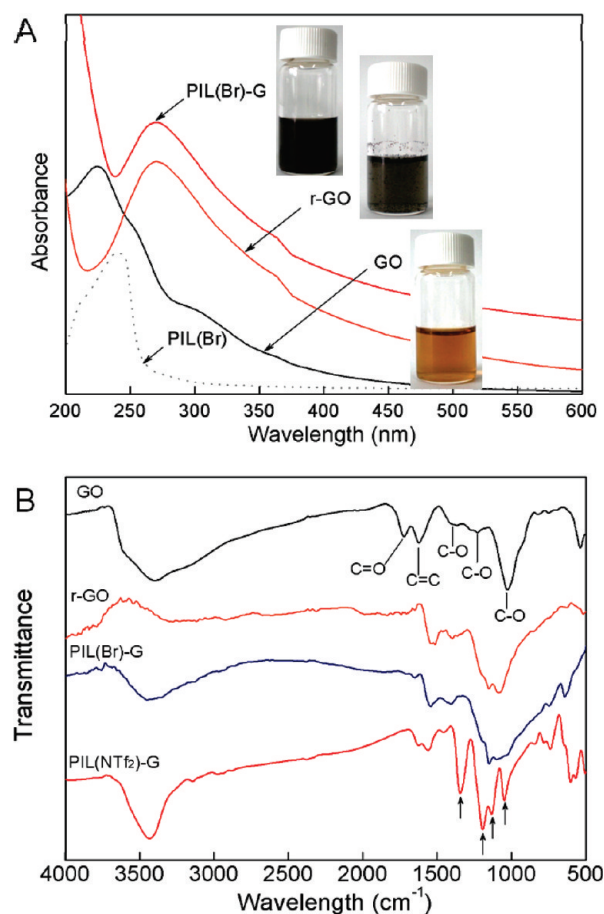


**Figure 2.** (a) UV-vis spectra and (b) FT-IR spectra of GO, reduced GO (r-GO), an aqueous suspension of PIL(Br)-G, and an organic phase suspension of PIL(NTf<sub>2</sub>)-G. In FT-IR spectra, the band appearances that are marked as arrows correspond to the NTf<sub>2</sub> anion of the PIL.

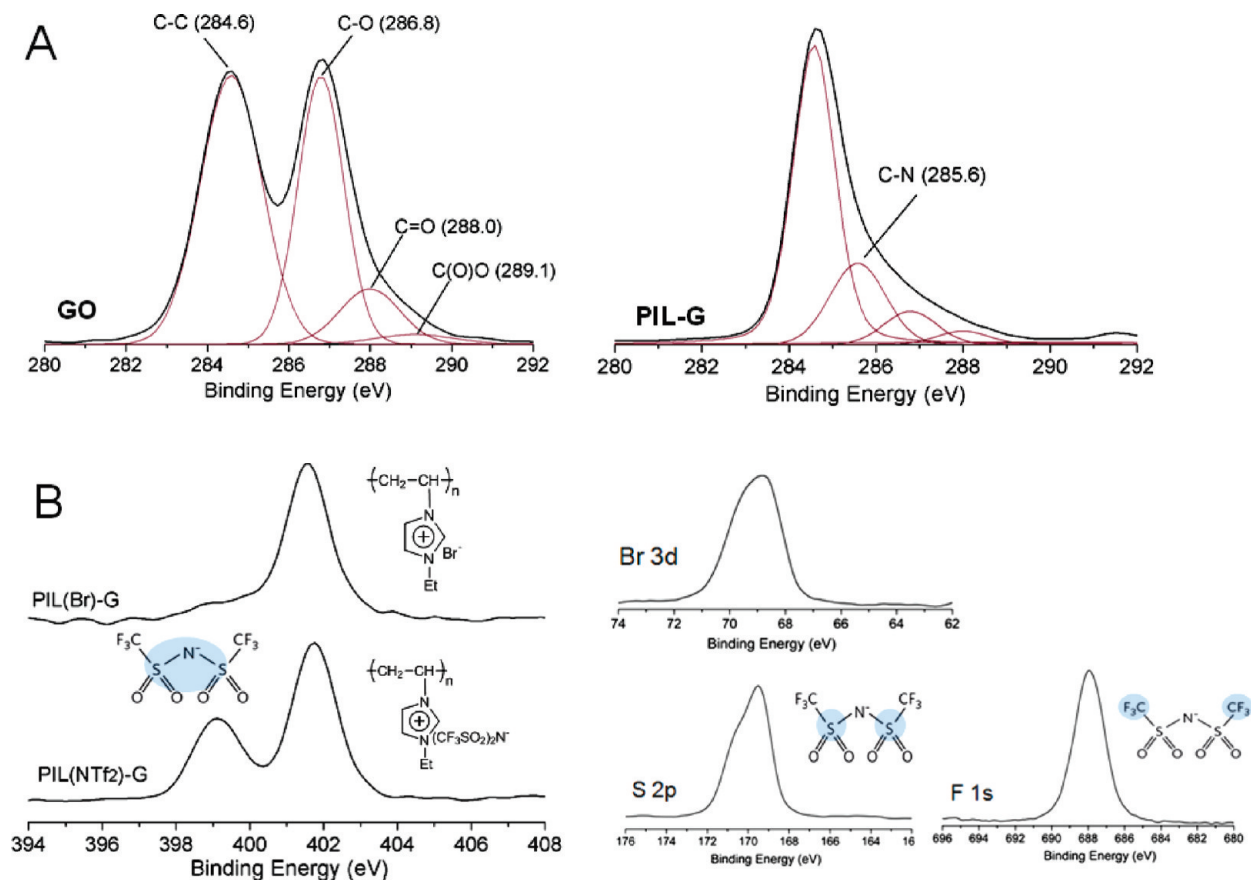


Figure 3. (A) Carbon 1s XPS profile of GO (left) and PIL(Br)-G (right); (B) comparison of XPS profile between hydrophilic PIL(Br)-G (upper) and hydrophobic PIL(NTf<sub>2</sub>)-G (lower).

the restoration of  $\pi$ -conjugated network within the graphene sheets occurred upon chemical reduction,<sup>14</sup> and the presence of PIL(Br) does not change the degree of reduction, which is supported by the conductivity value of PIL(Br)-G sheets ( $\sim 36$  S/cm).

Fourier transform infrared (FT-IR) spectroscopy in Figure 2b gives the characteristic absorption of functional groups and organic molecules on the graphene sheets. The FT-IR spectra of GO sheets showed C=O ( $1725\text{ cm}^{-1}$ ), aromatic C=C ( $1621\text{ cm}^{-1}$ ), carboxy C–O ( $1382\text{ cm}^{-1}$ ), epoxide/ether C–O ( $1231\text{ cm}^{-1}$ ), and alkoxy/alkoxide C–O stretches ( $1027\text{ cm}^{-1}$ ). In comparison to the IR spectrum of GO, those for PIL(Br)-G showed a decrease in C=O and C–O stretch intensities, confirming deoxygenation of the graphene sheets after chemical reduction. Upon anion exchange of PILs, the appearance of new bands corresponding to the NTf<sub>2</sub> anion ( $1341, 1193, 1133, 1046\text{ cm}^{-1}$ ) was observed, indicating a successful anion exchange and formation of the corresponding hydrophobic PIL(NTf<sub>2</sub>)-G.

To monitor the composition of PIL-modified graphene sheets, we employed X-ray photoelectron spectroscopy (XPS). In Figure 3a, the C 1s XPS spectrum of GO clearly indicates a considerable degree of oxidation with four different components which can be deconvoluted into  $\text{sp}^2$ -hybridized C–C in aromatic ring (284.6 eV), C–O (286.8 eV), C=O (288.0 eV), and C(O)OH (289.1 eV).

The atomic percentage (atom %) for different carbon functional groups is calculated with respect to the total area of the C 1s peak. Our observation indicates that the majority of oxygen groups consists of C–O bonds (36 atom %) which come from epoxide/ether and hydroxyl groups in the basal plane, while C=O (10 atom %, carbonyl) and C(O)OH (3 atom %, carboxylic) are present primarily at the edges of GO sheets in lesser amount. In comparison to the C 1s spectrum of GO sheets, that of the PIL-G sample clearly exhibited an increase in the C–C component and corresponding decrease in C–O (8 atom %) and C=O (3 atom %) components, indicating the restoration of large domains of  $\pi$ -conjugated structure. Additionally, new component at 285.6 eV corresponding to carbon bound to nitrogen (C–N) was observed because of the functionalization of graphene sheets with N-atom containing PIL molecules, which is also observed in the N 1s XPS spectrum in Figure 3b (left). On the basis of the above results, we could conclude that the oxygen functional groups are partially removed by the chemical reduction and the reduced GO sheets are modified by PIL(Br), resulting in the formation of PIL(Br)-G sheets that are electrically conductive but also water-dispersible. After the phase transferring of PIL-G sheets through anion exchange process, a change in the N 1s XPS spectrum was observed with two distinctive peaks for the energeti-

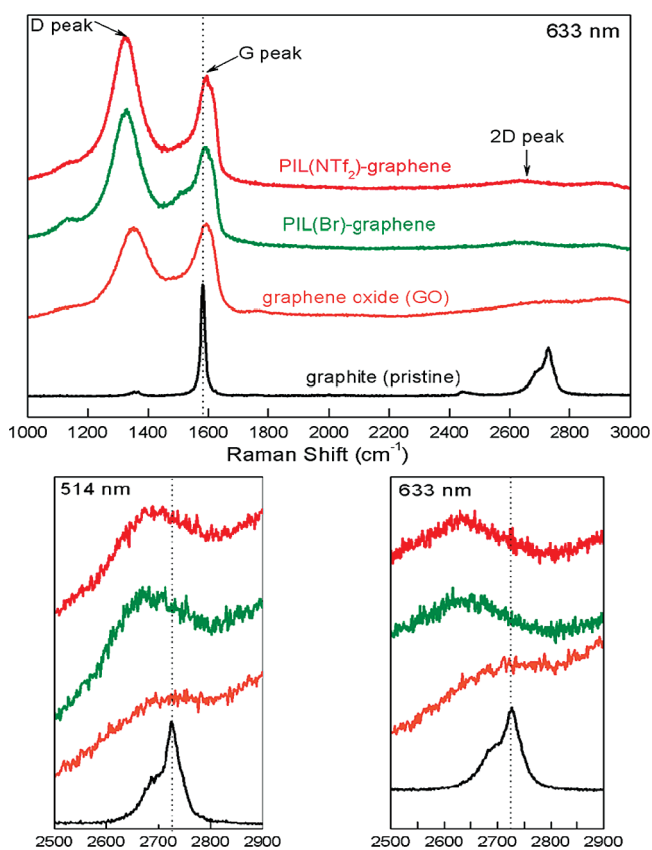


**Figure 4.** Raman spectra of pristine graphite, GO, PIL(Br)-G, and PIL(NTf<sub>2</sub>)-G.

cally well-separated imidazolium cation and the hydrophobic anion (NTf<sub>2</sub><sup>-</sup>) at 401.8 and 399.1 eV, respectively. The S 2p at 169.5 eV and F 1s at 687.9 eV also supports the presence of NTf<sub>2</sub><sup>-</sup> anions, confirming the successful anion exchange of the PIL and the formation of PIL(NTf<sub>2</sub>)-G.

During the chemical processing from pristine graphite to GO and then to the PIL-modified graphene sheets, graphene sheets are expected to undergo structural changes through the rearrangement of the carbon atoms in the basal plane. Such structural changes were monitored by Raman spectroscopy with a laser excitation of 514.5 and 632.8 nm, as shown in Figure 4. The studied film had been deposited on an alumina membrane by vacuum filtration and rinsed with water before drying. The Raman spectrum of the pristine graphite with 632.8 nm laser displays a prominent G peak at 1582 cm<sup>-1</sup> corresponding to the first-order scattering of the E<sub>2g</sub> mode, and 2D peak at 2726 cm<sup>-1</sup> originating from two phonon double resonance Raman process.<sup>25</sup> In the Raman spectrum of GO, the G peak is broadened and the D peak becomes prominent, indicating the reduction in size of the in-plane sp<sup>2</sup> domains possibly due to the extensive oxidation. The Raman spectrum of the PIL-modified graphene sheets are characterized by a presence of D (1324 cm<sup>-1</sup>), G (1591 cm<sup>-1</sup>), and 2D (2642 cm<sup>-1</sup>) peaks with an increased D/G intensity ratio compared to that in GO. This result suggests a creation of

new graphitic domains that are smaller in size but more numerous in number.<sup>12</sup> The intensities of 2D peaks with respect to the D and G peak are small due to disorder and they have been enlarged 10 times to demonstrate the shift between pristine graphite and PIL-modified graphene sheets. The shift in this peak can be used to estimate the number of layers in graphene sheets.<sup>25,26</sup> In the lower panels in Figure 4, the 2D bands of pristine graphite, GO, and PIL-modified graphene sheets are compared, in which the 2D peak positions in PIL-G are shifted considerably to a lower wavenumber by more than 50 cm<sup>-1</sup>. This result seems to indicate a decrease in the number of layers in PIL-modified graphene products, mainly due to the effective stabilization of graphene sheets with PIL during the reduction process. However, broad 2D peak of PIL-G with full width at half-maximum (fwhm) of approximately 130 cm<sup>-1</sup>, which is comparable to the result from other research groups,<sup>26</sup> makes an exact identification of the number of layers difficult. We suggest this feature is dominated by edge effects as the Raman excitation beam spot size of ~1.5 μm is larger than most of the graphene sheets, while we cannot rule out the possibility that some of graphene sheets were reaggregated during filtration in sample preparation. Nevertheless, the shape and position of 2D bands appears to be characteristic of thin graphitic platelets composed of less than five layers by comparison to other literature.<sup>26</sup>

From all previous results, we have shown that PILs promote the effective stabilization of the reduced GO sheets in water and/or organic solvents by the favorable interaction with the graphene sheets. Given the carboxyl acid groups at the edges of GO sheets, we suggest that the interaction of imidazolium cations in PIL with the carboxylic acid groups at the edges of GO sheets would be strong *via* electrostatic attractions. Therefore, parts of imidazolium cations in the PIL chain function to bind and stabilize the GO sheets, while the rest of imidazolium cations coupled with anions renders them dispersible in water and then in organic solvents upon the phase transfer process. Other possible interactions between PIL and graphene sheets may include the cation-π and/or π-π interactions, which were reported to be the case for PIL-functionalized carbon nanotubes.<sup>24</sup> Although the exact mechanism for the interaction between PIL and graphene sheets needs to be elucidated, it is clear that the GO sheets are functionalized with PIL and the interaction between them could be stable against chemical reduction by hydrazine. Therefore, the strong π-π and van der Waals interaction between graphene layers are shielded by PIL, which eventually prevent the agglomeration of the graphene sheets during the reduction process.

## CONCLUSIONS

This work demonstrated an effective approach for the preparation of solution-processable graphene sheets that were readily transferred between the aqueous and organic phases using PIL as the transferring vehicle. Chemically converted graphene sheets decorated with PIL were found to be stable against the chemical reduction and well dispersed in aqueous phase without any agglomera-

tion. The reversible hydrophilic-to-hydrophobic switching of graphene sheets was possible by simply exchanging the anions associated with PIL. The method enabled the use of low-cost solution processing techniques to apply graphene-based materials in large quantities. This approach will open up enormous opportunities that take advantage of the unique properties of graphene for many technological applications.

## METHOD

**Preparation of Graphene Oxide and Ionic Liquid Polymers (PIL).** Graphite oxide was synthesized from graphite flakes using the modified Hummel procedure.<sup>26,27</sup> Briefly, flake graphite (Bay Carbon SP-1, 5 g) was vigorously stirred in a solution of  $\text{KMnO}_4$  (25 g) in concentrated  $\text{NaNO}_3$  (3.75 g) and  $\text{H}_2\text{SO}_4$  (170 mL), washed with deionized water, and reacted with a 30 wt % aqueous solution of  $\text{H}_2\text{O}_2$  to complete the oxidation. The inorganic anions and other impurities were removed through repeated cycles of centrifugation, removal of the supernatant, and resuspension of the solid using an HCl solution. The resulting powder was suspended in water using ultrasonication and centrifuged at 10 000 rpm for 30 min to remove the multilayered species, which constituted ~15% of the powder by weight. The supernatant was an aqueous suspension of GO with a concentration of  $1.5 \text{ mg mL}^{-1}$  and was stable against precipitation. To prepare the PIL, poly(1-vinyl-3-ethylimidazolium) bromide was synthesized according to a previously reported procedure.<sup>22,28</sup> The PIL had a polymeric form with a weight average molecular weight ( $M_w$ ) of ~170 000 which was analyzed using gel permeation chromatography (GPC).

**Preparation of PIL-Functionalized Graphene Suspension.** To prepare the PIL-functionalized graphene dispersion, 400 mg (1.97 mmol, repeating unit) of PIL(Br) were dissolved in water and added to 19 mL ( $1.5 \text{ mg mL}^{-1}$ ) of an aqueous GO suspension. This mixture was then reduced with hydrazine monohydrate ( $16.5 \mu\text{L}$ , 3.2 mmol) at 90 °C for 1 h under continuous stirring. After reduction, a dispersion of reduced graphene oxide was centrifuged to yield a stable black supernatant, which was filtered through a Teflon membrane (0.2  $\mu\text{m}$  pore size) to produce an aqueous graphene suspension consisting of PIL(Br)-G.

**Phase Transfer Process.** An aqueous suspension of PIL(Br)-G was subjected to a phase transfer process with lithium bis(trifluoromethylsulfonyl) amide ( $\text{Li}^+ \text{NTf}_2^-$ ). First, 1.2 equiv of  $\text{NTf}_2^-$  with respect to the repeating units of PIL cations was added to complete the anion exchange reaction of PIL. Immediately after the addition of  $\text{Li}^+ \text{NTf}_2^-$  into the aqueous suspension of PIL(Br)-G, hydrophilic  $\text{Br}^-$  was substituted with hydrophobic  $\text{NTf}_2^-$ , resulting in dark black precipitates. The resulting PIL( $\text{NTf}_2$ )-G showed a range of solubility in polar aprotic solvents such as propylene carbonate (PC), dimethylformamide (DMF), acetonitrile (AN), tetrahydrofuran (THF), *N*-methyl-pyrrolidone (NMP), and nitromethane (NM). For phase transfer of graphene sheets from organic to water phase, 1.5 equiv of tetrabutylphosphonium bromide (TBPB) was added to the PIL( $\text{NTf}_2$ )-G suspension, creating a dark precipitate that was readily dispersible in water.

**Characterization.** The TEM images were taken with TECNAI 20 microscope by dispersing the graphene sheets in water or organic solvents, placing a few drops of the dispersion on a copper grid, and evaporating them prior to observation. Samples were prepared for the AFM measurements by depositing the corresponding suspension of PIL-G on the silicon wafer, drying it in vacuo, and investigating it using a AFM XE-100 (Park System) equipped with a tapping probe with reflex coating. The XPS measurements were performed with ESCA 2000 system (VG Microtech) using a monochromatized aluminum  $\text{K}\alpha$  anode. The Raman spectra were obtained using a Raman spectrometer (Jobin-Yvon, LabRam HR) equipped with an Ar-ion laser of 514.5 nm and He-Ne laser of 632.8 nm. The UV-vis spectra were ob-

tained using a Mecasys optizen 2120 UV spectrometer at room temperature, and FTIR spectra were recorded using a Nicolet 730 FT-IR spectrometer.

**Acknowledgment.** This work was supported by InsCon Tech, Co. Ltd, Korea. We thank Prof. Rodney S. Ruoff in the University of Texas at Austin for helpful discussion.

## REFERENCES AND NOTES

- Geim, A. K.; Novoselov, K. S. The Rise of Graphene. *Nat. Mater.* **2007**, *6*, 183–191.
- Novoselov, K. S.; Geim, A. K.; Morozov, S. V.; Jiang, D.; Zhang, Y.; Dubonos, S. V.; Grigorieva, I. V.; Firsov, A. A. Electric Field Effect in Atomically Thin Carbon Films. *Science* **2004**, *306*, 666–669.
- Gilje, S.; Han, S.; Wang, M.; Wang, K. L.; Kaner, R. B. A Chemical Route to Graphene for Device Applications. *Nano Lett.* **2007**, *7*, 3394–3398.
- Schedin, F.; Geim, A. K.; Morozov, S. V.; Hill, E. W.; Blake, P.; Katsnelson, M. I.; Novoselov, K. S. Detection of Individual Gas Molecules Adsorbed on Graphene. *Nat. Mater.* **2007**, *6*, 652–655.
- Lee, C.; Wei, X.; Kysar, J. W.; Hone, J. Measurement of the Elastic Properties and Intrinsic Strength of Monolayer Graphene. *Science* **2008**, *321*, 385–388.
- Balandin, A. A.; Ghosh, S.; Bao, W.; Calizo, I.; Teweldebrhan, D.; Miao, F.; Lau, C. N. Superior Thermal Conductivity of Single-Layer Graphene. *Nano Lett.* **2008**, *8*, 902–907.
- Bolotin, K. I.; Sikes, K. J.; Jiang, Z.; Klima, M.; Fudenberg, G.; Hone, J.; Kim, P.; Stormer, H. L. Ultrahigh Electron Mobility in Suspended Graphene. *Solid State Commun.* **2008**, *146*, 351–355.
- Stoller, M. D.; Park, S.; Zhu, Y.; An, J.; Ruoff, R. S. Graphene-Based Ultracapacitors. *Nano Lett.* **2008**, *8*, 3498–3502.
- McAllister, M. J.; Li, J.-L.; Adamson, D. H.; Schniepp, H. C.; Abdala, A. A.; Liu, J.; Herrera-Alonso, M.; Milius, D. L.; Car, R.; Prud'homme, R. K.; *et al.* Single Sheet Functionalized Graphene by Oxidation and Thermal Expansion of Graphite. *Chem. Mater.* **2007**, *19*, 4396–4404.
- Berger, C.; Song, Z. M.; Li, X. B.; Wu, X. S.; Brown, N.; Naud, C.; Mayou, D.; Li, T.; Hass, J.; Marchenkov, A. N.; *et al.* Electronic Confinement and Coherence in Patterned Epitaxial Graphene. *Science* **2006**, *312*, 1191–1196.
- Wang, X.; Zhi, L.; Tsao, N.; Tomovic, Z.; Li, J.; Müllen, K. Transparent Carbon Films as Electrodes in Organic Solar Cells. *Angew. Chem., Int. Ed.* **2008**, *47*, 2990–2992.
- Stankovich, S.; Dirkin, D. A.; Piner, R. D.; Kohlhaas, K. A.; Kleinhammes, A.; Jia, Y.; Wu, Y.; Nguyen, S. T.; Ruoff, R. S. Synthesis of Graphene-Based Nanosheets via Chemical Reduction of Exfoliated Graphite Oxide. *Carbon* **2007**, *45*, 1558–1565.
- Stankovich, S.; Dirkin, D. A.; Dommett, G. H. B.; Kohlhaas, K. M.; Zimney, E. J.; Stach, E. A.; Piner, R. D.; Nguyen, S. T.; Ruoff, R. S. Graphene-Based Composite Materials. *Nature* **2006**, *442*, 282–286.
- Li, D.; Müller, M. B.; Gilje, S.; Kaner, R. B.; Wallace, G. G. Processable Aqueous Dispersions of Graphene Nanosheets. *Nat. Nanotechnol.* **2008**, *3*, 101–105.

15. Stankovich, S.; Piner, R. D.; Chen, X. Q.; Wu, N. Q.; Nguyen, S. T.; Ruoff, R. S. Stable Aqueous Dispersions of Graphitic Nanoplatelets via the Reduction of Exfoliated Graphite Oxide in the Presence of Poly(sodium 4-styrenesulfonate). *J. Mater. Chem.* **2006**, *16*, 155–158.
16. Xu, Y.; Bai, H.; Lu, G.; Li, C.; Shi, G. Flexible Graphene Films via the Filtration of Water-Soluble Noncovalent Functionalized Graphene Sheets. *J. Am. Chem. Soc.* **2008**, *130*, 5856–5857.
17. Patil, A. J.; Vickery, J. L.; Scott, T. B.; Mann, S. Aqueous Stabilization and Self-Assembly of Graphene Sheets into Layered Bio-nanocomposites Using DNA. *Adv. Mater.* **2009**, *21*, 3159–3164.
18. Hernandez, Y.; Nicolosi, V.; Lotya, M.; Blighe, F. M.; Sun, Z.; De, S.; McGovern, I. T.; Holland, B.; Byrne, M.; Gun'ko, Y. K.; *et al.* High-Yield Production of Graphene by Liquid-Phase Exfoliation of Graphite. *Nat. Nanotechnol.* **2008**, *3*, 563–568.
19. Blake, P.; Brimicombe, P. D.; Nair, R. R.; Booth, T. J.; Jiang, D.; Schedin, F.; Ponomarenko, L. A.; Morozov, S. V.; Gleeson, H. F.; Hill, E. W.; *et al.* Graphene-Based Liquid Crystal Device. *Nano Lett.* **2008**, *8*, 1704–1708.
20. Liu, N.; Luo, F.; Wu, H.; Liu, Y.; Zhang, C.; Chen, J. One-Step Ionic-Liquid-Assisted Electrochemical Synthesis of Ionic-Liquid-Functionalized Graphene Sheets Directly from Graphite. *Adv. Funct. Mater.* **2008**, *18*, 1518–1525.
21. Lu, J.; Yang, J.; Wang, J.; Lim, A.; Wang, S.; Loh, K. P. One-Pot Synthesis of Fluorescent Carbon Nanoribbons, Nanoparticles, and Graphene by the Exfoliation of Graphite in Ionic Liquids. *ACS Nano* **2009**, *3*, 2367–2375.
22. Marcilla, R.; Ochoteco, E.; Pozo-Gonzalo, C.; Grande, H.; Pomposo, J. A.; Mecerreyes, D. New Organic Dispersions of Conducting Polymers Using Polymeric Ionic Liquids as Stabilizers. *Macromol. Rapid Commun.* **2005**, *26*, 1122–1126.
23. Kim, T.; Suh, M.; Kwon, S. J.; Lee, T. H.; Kim, J. E.; Lee, Y. J.; Kim, J. H.; Hong, M.; Suh, K. S. Poly(3,4-ethylenedioxythiophene) Derived from Poly(ionic liquid) for the Use as Hole-Injecting Material in Organic Light-Emitting Diodes. *Macromol. Rapid Commun.* **2009**, *30*, 1477–1482.
24. Marcilla, M.; Curri, M. L.; Cozzoli, P. D.; Martínez, M. T.; Loinaz, I.; Grande, H.; Pomposo, J. A.; Mecerreyes, D. Nano-objects on a Round Trip from Water to Organics in a Polymeric Ionic Liquid Vehicle. *Small* **2006**, *2*, 507–512.
25. Ferrari, A. C.; Meyer, J. C.; Scardaci, V.; Casiraghi, C.; Lazzeri, M.; Mauri, F.; Piscanec, S.; Jiang, D.; Novoselov, K. S.; Roth, S.; *et al.* Raman Spectrum of Graphene and Graphene Layers. *Phys. Rev. Lett.* **2006**, *97*, 187401.
26. Eda, G.; Fanchini, G.; Chhowalla, M. Large-Area Ultrathin Films of Reduced Graphene Oxide as a Transparent and Flexible Electronic Material. *Nat. Nanotechnol.* **2008**, *3*, 270–274.
27. Hummers, W. S.; Offerman, R. E. Preparation of Graphitic Oxide. *J. Am. Chem. Soc.* **1958**, *80*, 1339.
28. Kim, T. Y.; Lee, T. H.; Kim, J. E.; Kasi, R. M.; Sung, C. S. P.; Suh, K. S. Organic Solvent Dispersion of Poly(3,4-ethylenedioxythiophene) with the Use of Polymeric Ionic Liquid. *J. Polym. Sci., Part A* **2008**, *46*, 6872–6879.